Performance Control of Three-Phase Induction Motor Operated From A Single-Phase Supply

Hamdy A. Ashour[1] and Yasser. G. Dessouky
Arab Academy for Science and Technology, Dept of Electrical and Control Engineering, P.B.1029, Miami, Alexandria, Egypt, [1]hashour@aast.edu

*Abstract*__ **This paper presents analytical and experimental performance and control of a three-phase induction motor fed from a single-phase supply via a single capacitor. The transient and steady state analysis are predicted using d-q model representation whose frame is chosen stationary. The value of capacitance to provide minimum unbalance ratio is theoretically calculated and is experimentally implemented using Fixed Capacitor-Thyristor Controlled Reactor (FC-TCR) scheme applied for large induction motors. The speed is controlled using a TRIAC coupled in series with the supply. The dynamic model is introduced and both simulated and experimental waveforms are predicted. This is applied for a fractional horsepower fan drive.**

List of symbols

R_s , R_r	: stator and rotor resistances
M , L_s , L_r	: mutual and stator and rotor self inductance
i_{ds} , i_{qs}	: instantaneous d-q stator currents
i_{dr} , i_{qr}	: instantaneous d-q rotor currents
v_{ds} , v_{qs}	: instantaneous d-q stator voltages
v_{dr} , v_{qr}	: instantaneous d-q rotor voltages
v_{as}, v_{bs}, v_{cs}	: instantaneous abc stator voltages
v_s ,v_c	: supply and capacitor voltages
i_s , i_c	: supply and capacitor currents
s , ω_s , ω_r	: slip. synchronous and rotor speeds
P , J	: no. of poles and moment of inertia
p , j	: differential and complex operators
X_c , C	: balance reactance and capacitance
T_L , T_e	: Load torque and motor developed torque
V_s , I_s	: RMS supply voltage and current
V_{ds} , V_{qs}	: RMS d-q stator voltages
I_{qs} , I_{ds}	: RMS d-q stator currents
I_{qr} , I_{dr}	: RMS d-q rotor currents
α , dt	: delay angle of the thyristor and time step
L_α , C_α	: inductance and capacitance of FC-TCR
i_L	: current in inductance L_α
UR%	: minimum unbalance ratio
P_s , P_L	: instantaneous supply and FCTCR power
Φ_s	: supply voltage and current phase difference

I. INTRODUCTION

Three-phase induction motor (IM) may be operated from a 1-ph supply according to the available supply. Many researches have been carried out to explain and analyze this operation [1-6]. However, in many industrial applications, a variable speed output from 3-ph induction motor is necessary with minimum unbalance operation. This paper presents a transient and steady state analysis using d-q model representation for a 3-ph IM fed from a 1-ph ac supply via one capacitor as shown in fig. (1-a). The effect of the capacitor on the performance is studied. The Fixed Capacitor-Thyristor Controlled Reactor (FC-TCR) scheme is implemented to ensure minimum unbalance ratio. This is better applied for large induction motors where the acoustic noise and motor efficiency are considered. Also, the speed control of a fractional hp fan drive using a traic in series with the supply is presented.

II. ANALYSIS AND DYNAMIC EQUATIONS

The equations describing the performance of the machine shown in fig. (1-a) can be derived using d-q model representation where d and q axes are chosen stationary in space.

Transformation from 3-ph abc to dq variables may be written as [7]:

$$\begin{bmatrix} X_{as} \\ X_{bs} \\ X_{cs} \end{bmatrix} = \begin{bmatrix} 1 & 0 \\ -1/2 & \sqrt{3}/2 \\ -1/2 & -\sqrt{3}/2 \end{bmatrix} \begin{bmatrix} X_{ds} \\ X_{qs} \end{bmatrix} \quad (1)$$

where variable X represents current or voltage. The voltage-current relations for stator and rotor dq phases are derived from basic principles and given by [7]:

$$p i_{dq} = \left[L_{dq}\right]^{-1} v_{dq} \quad (2)$$

where

$$L_{dq} = \begin{bmatrix} L_s & 0 & M & 0 \\ 0 & L_s & 0 & M \\ M & 0 & L_r & 0 \\ 0 & M & 0 & L_r \end{bmatrix}, i_{dq}^T = \begin{bmatrix} i_{ds} & i_{qs} & i_{dr} & i_{qr} \end{bmatrix}^T$$

, and $v_{dq} = \begin{bmatrix} v_{ds} - R_s i_{ds} \\ v_{qs} - R_s i_{qs} \\ -R_r i_{dr} + \omega_r \left(M i_{qs} + L_r i_{qr}\right) \\ -R_r i_{qr} - \omega_r \left(M i_{ds} + L_r i_{dr}\right) \end{bmatrix}$

From the connection and phase diagram of fig (1-a), it is seen that:

$$\left.\begin{aligned} v_s &= v_{as} \\ v_c &= -v_{bs} \\ p v_c &= \frac{i_c}{C} \\ i_c &= i_{bs} - i_{cs} \\ i_s &= i_{as} - i_{cs} \end{aligned}\right\} \quad (3)$$

Substituting by (1) into (3) and rearranging, yields:

$$v_{ds} = v_s \quad (4)$$

$$p v_c = \frac{\sqrt{3}}{C} i_{qs} \quad (5)$$

$$v_{qs} = \frac{1}{\sqrt{3}} v_{ds} - \frac{2}{\sqrt{3}} v_c \quad (6)$$

$$i_s = \frac{3}{2} i_{ds} + \frac{\sqrt{3}}{2} i_{qs} \quad (7)$$

Moreover, the instantaneous electromagnetic torque, can be expressed in terms of d-q stator and rotor currents as :

$$T_e = \left(\frac{3}{2}\right)\left(\frac{P}{2}\right) M \left(i_{qr} i_{ds} - i_{dr} i_{qs}\right) \tag{8}$$

The mechanical equation of the machine is given by:

$$p\omega_r = \left(\frac{1}{J}\right)\left(\frac{P}{2}\right)\left(T_e - T_L\right) \tag{9}$$

Equations (2) and (4) to (9) represent the dynamic model of the machine. Knowing the supply voltage, capacitance and load torque and assuming zero initial condition for speed, capacitor voltage and dq currents, the transient response of the machine can be predicted.

III. STEADY STATE ANALYSIS

The dynamic model derived in section (II) may also predict the steady state analysis of the machine as shown in fig. (1-b) by substituting $(1-s)\omega_s$ for ω_r and 'j' for 'p'. This can be written as:

$$\left.\begin{aligned} [\bar{I}] &= [\bar{Z}]^{-1}[\bar{V}] \\ \bar{V}_{ds} &= V_s \angle 0 \\ \bar{V}_{qs} &= \bar{V}_{ds} + 2jX_c \bar{I}_{qs} \\ \bar{I}_s &= \frac{3}{2}\bar{I}_{ds} + \frac{\sqrt{3}}{2}\bar{I}_{qs} \end{aligned}\right\} \tag{10}$$

where

$$\bar{Z} = \begin{bmatrix} \bar{Z}_s & 0 & jX_m & 0 \\ 0 & \bar{Z}_s - 2jX_c & 0 & jX_m \\ jX_m & -(1-s)X_m & \bar{Z}_r & -(1-s)X_r \\ (1-s)X_m & jX_m & (1-s)X_r & \bar{Z}_r \end{bmatrix}$$

$$[\bar{V}]^T = \left[V_s \angle 0 \quad \frac{V_s}{\sqrt{3}}\angle 0 \quad 0 \quad 0\right]^T,$$

$$[\bar{I}]^T = \left[\bar{I}_{ds} \quad \bar{I}_{qs} \quad \bar{I}_{dr} \quad \bar{I}_{qr}\right]^T,$$

$$\bar{Z}_s = R_s + j\omega_s L_s\ ,\ \bar{Z}_r = R_r + j\omega_s L_r\ ,$$

$X_r = \omega_s L_r$, $X_m = \omega_s M$, and $X_c = \dfrac{1}{\omega_s C}$

Having got the d-q currents and voltages for a given operating condition consisting of supply voltage, speed and capacitance, the abc phase currents and voltages can be calculated from (1). The average torque, T_L and amplitude of double supply frequency oscillation torque, T_{osc} are derived from (8) and given by [8]:

$$\left.\begin{aligned} T_L &= \left(\frac{3}{2}\right)\left(\frac{P}{2}\right) M\ \text{real}\left(\bar{I}_{qr}\bar{I}_{ds}^{*} - \bar{I}_{dr}\bar{I}_{qs}^{*}\right) \\ T_{osc} &= \left(\frac{3}{2}\right)\left(\frac{P}{2}\right) M \left|\bar{I}_{qr}\bar{I}_{ds} - \bar{I}_{dr}\bar{I}_{qs}\right| \end{aligned}\right\} \tag{11}$$

The oscillation torque results in double frequency oscillation speed component

IV. EFFECT OF CAPACITANCE ON PERFORMANCE

It should be noted that the motor operates in an unbalanced mode. This means existence of double frequency pulsating torque in steady state. The choice of phase balancer capacitor may be analyzed to achieve minimum unbalance, minimum negative sequence voltage or zero negative sequence voltage, [9] or to achieve maximum output torque or maximum input power factor, [8] or to achieve minimum torque pulsation, [10]. In this analysis, the capacitor is choiced based on criteria of minimum unbalance ratio, UR% (negative sequence voltage component to positive sequence voltage component ratio), which is given by [11]:

$$UR\,\% = \left|\frac{V_{ds} + jV_{qs}}{V_{ds} - jV_{qs}}\right| \tag{12}$$

In the steady state model, for a given operating condition consisting of supply voltage and speed, the capacitance is changed using a trial and error method and for each value of capacitance, the unbalance ratio is calculated. This is repeated until the capacitance $C_{min\text{-}UR}$ that results in minimum unbalance is evaluated. The relationship between speed and both corresponding value of capacitance $C_{min\text{-}UR}$ and the unbalance ratio ,which is then minimum, is shown in fig. (2-a) and (2-b) respectively. Fig. (2) shows the steady state performance of a Δ-220V, 2.2kW, 4-pole, 50Hz machine, run at minimum unbalance ratio. The dynamic model can validated to conclude the transient response by choosing an operating point as shown in fig. (3). The machine starts at no load with electromechanical torque and speed pulsations while the phases' emf is building up. When the load is applied, the machine runs with minimum speed and torque pulsations and phases voltages are nearly equal. It should be noted that if the load is changed, the capacitance needs to be changed to resume minimum unbalance ratio.

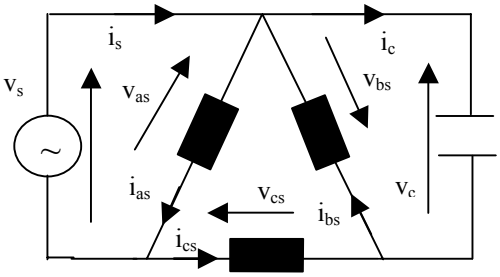

(a)

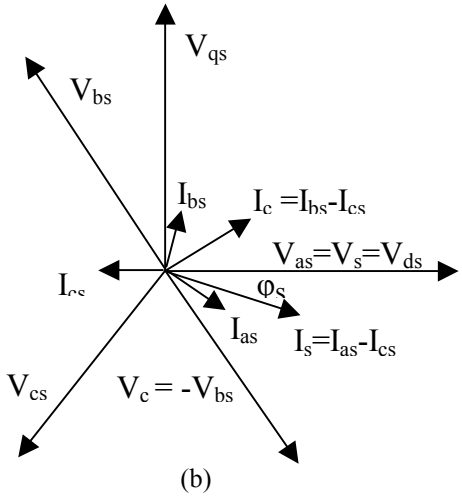

(b)

Fig. 1: (a) Connection diagram (b) phasor diagram

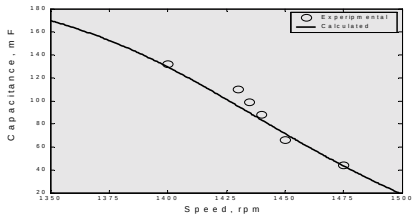

(a)

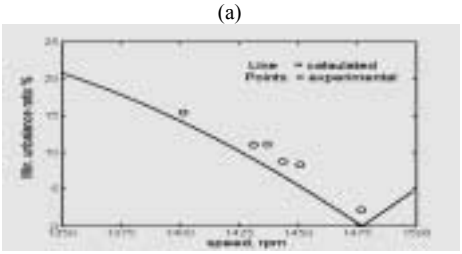

(b)

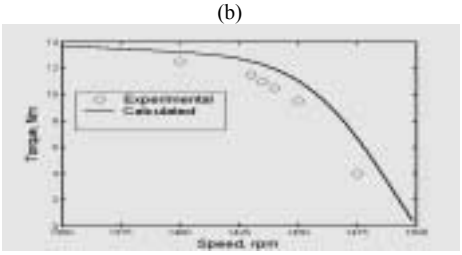

(c)

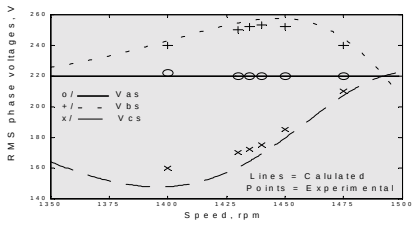

(d)

Fig. 2 Relationship between speed versus (a) $C_{min\text{-}UR}$ (b) UR% (c) torque (d) RMS phase voltages

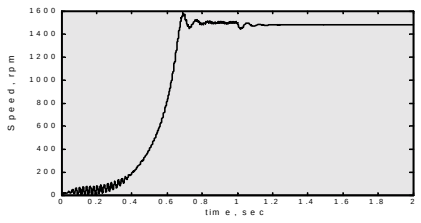

(a)

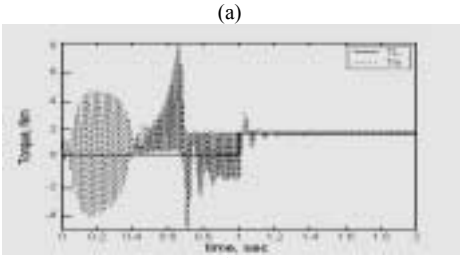

(b)

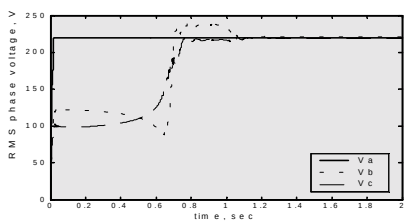

(c)

Fig. 3 Relationship between time versus (a) speed (b) torque and (c) phase voltages

V. MINIMUM UNBALANCE RATIO USING FC-TCR

As shown in fig. (2-a), a minimum unbalance ratio can be obtained by providing the required value of terminal capacitance for each speed. This is not practically important for small motors but useful for large motors where efficiency and acoustic noise occurred by the double supply frequency oscillations torque are considered. A smooth variation of capacitance can be obtained by using static exciter employing a Fixed Capacitor-Thyristor Controlled Reactor (FC-TCR) scheme, [12] as shown in fig. (4). If the reactance factor, which is the ratio between inductive to capacitive reactance is 'u'. Therefore, the value of the inductor, L_α is related to the maximum capacitance required, C_α and the factor, u is given by:

$$\omega_s L_\alpha = \frac{u}{\omega_s C_\alpha} \tag{13}$$

The lagging current taken by the inductor can be controlled smoothly by varying the delay angle of the traic, α, where ($0 \leq \alpha \leq \pi/2$) with respect to peak value of the capacitor voltage [12]. The effective value of the variable capacitance provided by the exciter is therefore given by:

$$C_{\min-UR} = C_\alpha \left[1 - \frac{1}{u\pi}\left(\pi - 2\alpha - \sin(2\alpha)\right) \right] \tag{14}$$

Therefore, $C_{min\text{-}UR}$ changes from C_α (1 - 1/u) to C_α as the angle, α changes from 0 to π/2 respectively. To conclude a simulation of this drive, the model is derived both when the traic is on (ON-STATE) and when it is off (OFF-STATE) as follows.

A. ON-STATE OF FC-TCR DRIVE

This period starts when a gate pulse is applied to the traic at a delay angle, α, with respect to peak value of capacitor voltage and continues up to π-α and repeats during the other half cycle during which the traic is on. The motor equations are as follows.

$$i_c + i_L = i_{bs} - i_{cs} \tag{15}$$

Substituting by (1) into (15), yields:

$$i_c = \sqrt{3} i_{qs} - i_L \tag{16}$$

Also it seen that:

$$p i_L = \frac{v_c}{L_\alpha} \tag{17}$$

B. OFF-STATE OF FC-TCR DRIVE

This period continues between π-α up to π+α and repeats in the other half cycle during which the TRIAC is off. The equations during this period resemble those of section (II).

C. SIMULATION AND RESULTS

For the 2.2 kW motor, and as shown in fig. (2-a), as the speed changes from 1350 rpm to 1500 rpm, the capacitance $C_{min\text{-}UR}$ changes from 170 μF to 19 μF. Therefore, the capacitance, C_α is taken 170 μF and consequently, the inductor L_α and the reactance factor, u

will be 67 mH and 1.126 as calculated from (13) and boundary limits of (14) respectively. The model of this drive can be predicted as shown in the flow chart of fig. (5) and the results are shown in fig. (6) and (7). The motor is started at no load and then the load is applied at time, t_1 during which the machine runs in an unbalanced mode. The firing delay angle of the FC-TCR is adjusted at time, t_2, as shown in fig. (6) to obtain minimum unbalance ratio. This can be noticed from the motor speed and torque waveforms. The steady state waveform of capacitor current and voltage after time t_2 is shown in fig.(7).

VI. SPEED CONTROL OF THE MACHINE

Varying the supply voltage results in controlling the speed of the induction machine. This can be achieved using a traic as shown in fig. (8). Varying the delay angles of the traic effectively changes the applied voltage to the machine. A closed loop control circuit has little practical importance. However, for a fractional horsepower fan drive, an open loop speed control may be used. To predict the machine performance, the model of the machine is derived both when the traic is on (ON-STATAE) and when it is off (OFF-STATE) as follows.

A. ON-STATE OF SPEED CONTROL DRIVE

This period starts when a gate pulse is applied to the traic at a delay angle, α, with respect to zero crossing of supply voltage positive half cycle up to π but due to inductive nature of the motor, the traic continues to conduct where the power, P_s, is recovered from the motor to the supply until supply current falls to zero at an extinction angle, γ approximately equals $\pi+\Phi_s$ [11] before which the gate pulse for the negative half cycle is applied at π+α to avoid asymmetrical waveform of motor voltage and current, (i.e. $\pi+\Phi_s \approx \gamma < \pi+\alpha$) or ($\Phi_s < \alpha$). This is practically ensured by applying continuous gate signal from α to π. Therefore, the delay angle, α is controlled in the range between Φ_s (which is load dependent) at which the motor voltage equals the supply voltage and up to π at which motor voltage is zero [11]. The same applies for the negative half cycle. The motor equations during this period are the same as detailed in section (II).

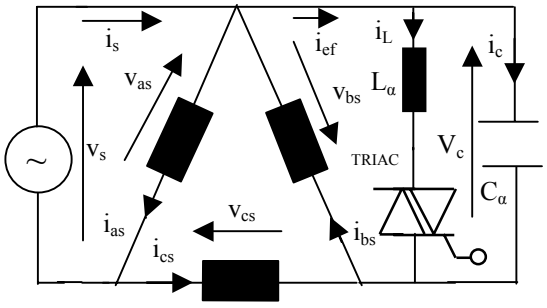

Fig. 4 Connection diagram of a IM drive supply using FCTCR

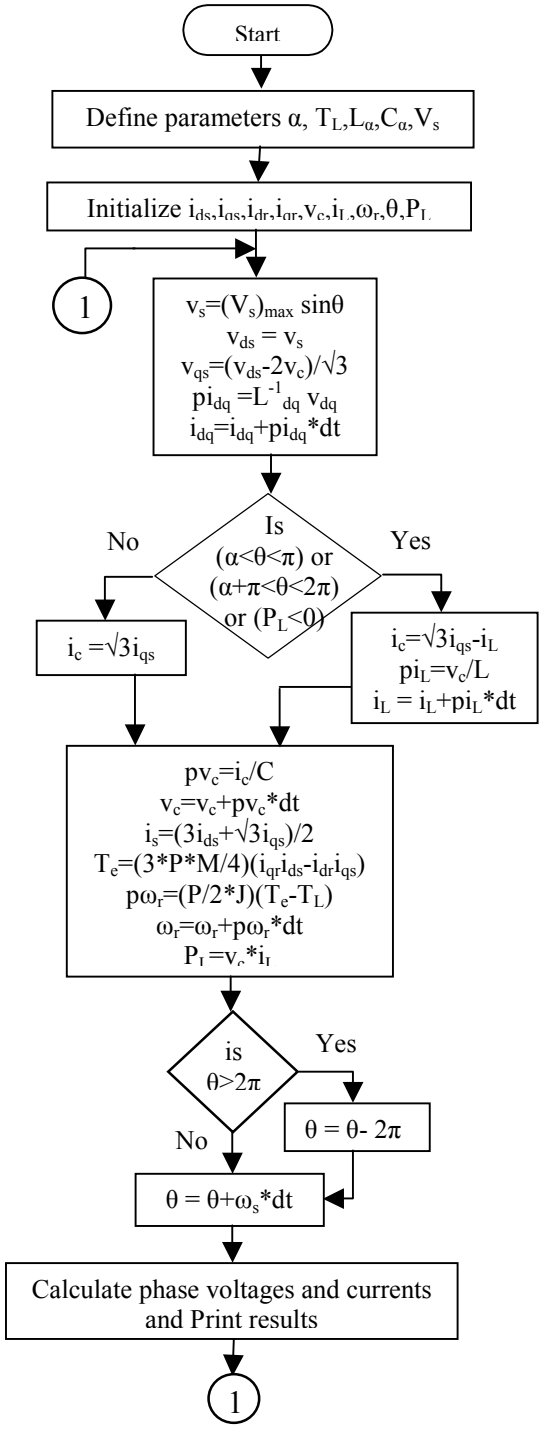

Fig. 5 Flow chart of FC_TCR drive

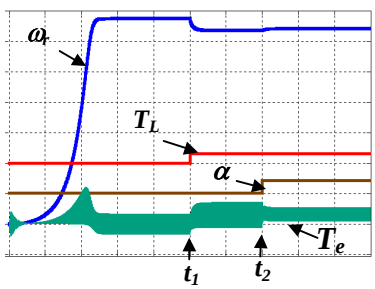

Fig. 6 Effect of FC-TCR firing angle on motor (ω_r) 215 rpm/div (T_L) 15 Nm/div (α) 180^0/div (T_e) 15 Nm/div (horizontal) 1 Sec/div

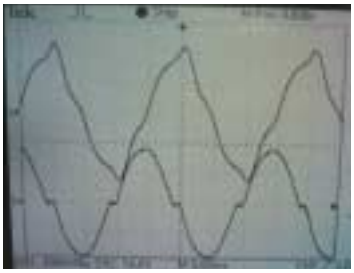

(a)

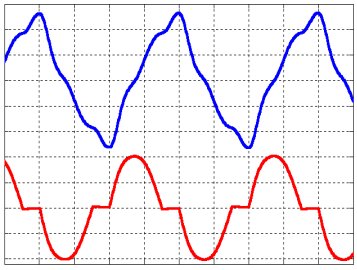

(b)

Fig. 7 Voltage and current of the FC-TCR connected to the 3-ph motor
(a) Experimental (b) Simulated
(upper) v_c [100V/div] (lower) i_{ef} [3 A/div]
(horizontal) t [5 mSec/div]

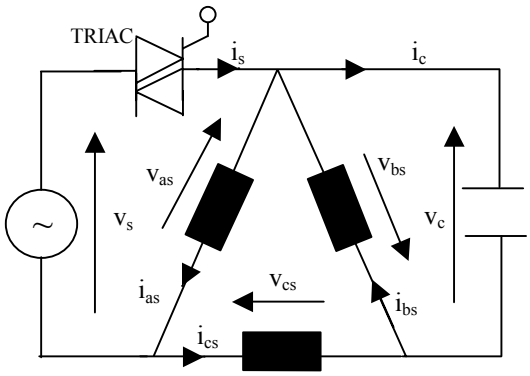

Fig. 8 Connection diagram of a 3-ph IM fed from a 1-ph supply via a TRIAC using a capacitor

B. OFF-STATE OF SPEED CONTROL DRIVE

This period continues between the extinction angle, γ, till the gate signal is applied at π+α during which the TRIAC is off and as a result the supply current, i_s, is zero. With reference to (3), this implies that:

$$i_{as} = i_{cs} \tag{18}$$

Substituting by (1) into (18) to get:

$$i_{ds} = -\frac{1}{\sqrt{3}} i_{qs} \tag{19}$$

Then substituting by (19) into (4) and rearranging yields:

$$pi_{off} = \left[L_{off}\right]^{-1} v_{off} \tag{20}$$

where,

$$L_{off} = \begin{bmatrix} L_s & 0 & M \\ -\frac{M}{\sqrt{3}} & L_r & 0 \\ M & 0 & L_r \end{bmatrix}, \quad i_{off}^T = \begin{bmatrix} i_{qs} & i_{dr} & i_{dr} \end{bmatrix}^T$$

, and $v_{off} = \begin{bmatrix} v_{qs} - R_s i_{qs} \\ -R_r i_{dr} + \omega_r \left(M i_{qs} + L_r i_{qr}\right) \\ -R_r i_{qr} - \omega_r \left(-\frac{M}{\sqrt{3}} i_{qs} + L_r i_{dr}\right) \end{bmatrix}$

Also from (4), it is seen that:

$$v_{ds} = R_s i_{ds} + L_s \; pi_{ds} + M \; pi_{dr} \tag{21}$$

Then (5) to (9) are also valid during this OFF-STATE.

C. SIMULATION AND RESULTS

The flow chart of the drive simulation using Euler's method to solve differential equations is shown in fig. (9). Fig. (10) shows the effect of changing the TRIAC delay angle on the speed. The machine is started at high value of delay angle to provide soft starting. It is noted that when the delay angle is less than 40º, which is the machine load angle at this loading condition, the delay angle has no effect on the speed as the current is continuous [11]. When the delay angle is increased from 40º to 140º, the speed reduces from 2950 rpm to 2200 rpm (i.e.: 25%). Fig. (11) shows the instantaneous waveform of the supply current and voltage across phase ab of the machine at steady state as obtained from experimental rig and simulated model respectively for a Y-220V, 500W, 2-pole, 50Hz machine.

VII. CONCLUSIONS

The performance and control of a 3-ph induction motor fed from a 1-ph supply via a capacitor is studied. The transient and steady state analysis are presented using a d-q model representation whose frame is chosen stationary. The effect of the capacitor on the steady state performance is discussed where the machine can run with minimum voltage unbalance ratio by proper choice of the capacitance. The FC-TCR scheme is theoretically analyzed and experientially applied to provide minimum unbalance ratio for large induction motors where acoustic noise is considered. The open loop control speed control of a fractional hp fan drive is suggested by varying the supply voltage using a traic. This is experimentally applied and theoretically investigated.

VIII. REFERENCES

[1] G.M. Hertz, 'Current techniques in phase conversion systems', IEEE Rural electric power conference, Minneopolis, Minnestota, May, 1978 pp 78-83.

[2] K. Jon,' An up to date look at conversion of single phase to three phase power', contactor electrical equipment (CEE), Jan., 1981.

[3] O. J. M. Smith, 'High efficiency single phase motor', IEEE Trans. on EC, vol.7, No.3, Sept. 1992, pp 560-569.

[4] O. J. M. Smith, 'Large low cost single phase semihex™ motors', IEEE Trans. on EC, vol.14, No.4, Dec. 1999, pp 1353-1358.

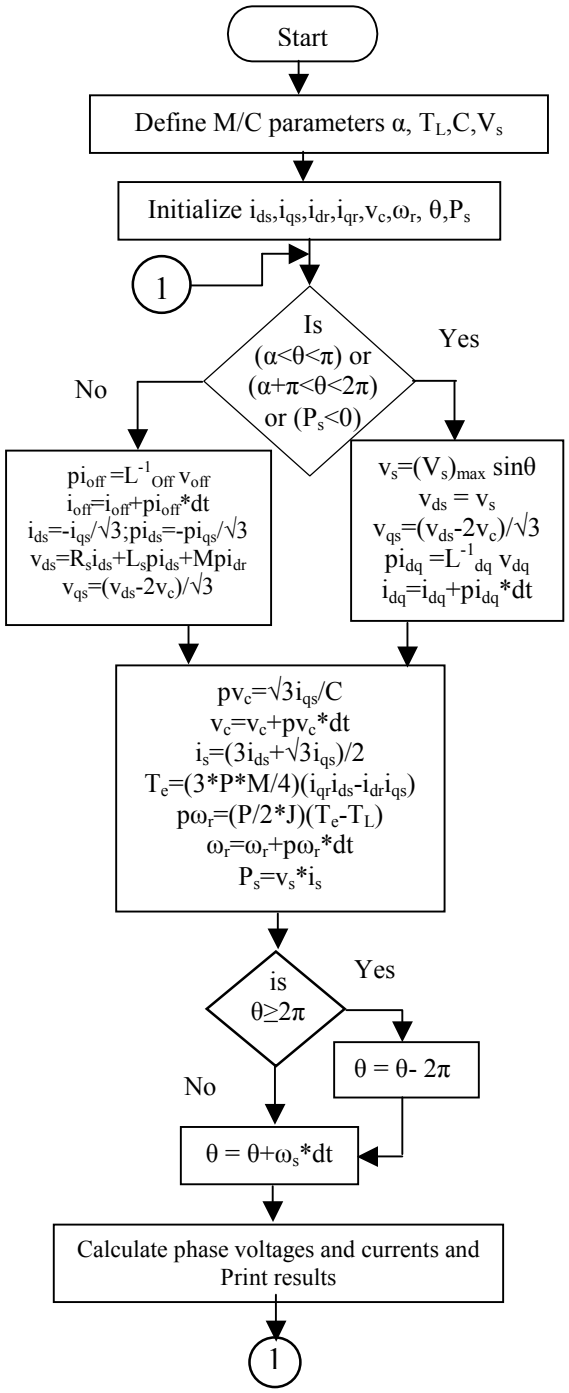

Fig. 9 Flow chart of speed control using a traic

[5] T. F. Chan, 'Single phase operation of a three phase induction generator with the Smith connection', IEEE Trans. on EC, vol.17, No.1, March. 2002, pp 47-54.

[6] S. S. Murthy et al, 'Transient analysis of a three phase induction motor with single phase supply', IEEE Trans. on PAS, PAS-102, 1983, pp 28-37.

[7] A.E. Fitzgerald and C. Kingsely,' Electric Machinary: the dynamics and statics of electromechanical energy conversion', Mc GrawHill Book Company, Inc, 5th edition, 1992.

[8] A.L. Mohamadein, A. Al-Ohaly and A.H. Al-Bahrani,,' On the choice of phase balancer capacitance for induction motors fed from 1-ph supply,' IEEE Trans., EC-2, 1987, pp 458-464.

[9] R.S. Jha and C.S. Jha,' Operation of 3-ph IM connected to a single phase supply system', Journal of the institution of Engineering (India), 58, pt. EL6, 1978, pp 339.

[10] Al-Ohaly, A.L. Mohamadein and A.H. Al-Bahrani, 'Effect of phase balancer capacitance on the dynamic behavior of a three phase induction motor operated from a single phase supply', J. King Saud Univ., Riyadh, Eng. Sci.(1,2), vol.1, 1989, pp 123-146.

[11] J. Handmarch,' Electric Machines and their application', Pergoman Press, 1976.

[12] M.B. Brennen and A.A. Abbaondanti, 'Static exciter for induction generators', IEEE Trans. on IA, vol. IA-13, No.5, 1977, pp 422-428.

[13] M.H. Rashid,' Power electronics: circuits, devices and applications', Prectice Hall International Editions, 2nd edition,1993.

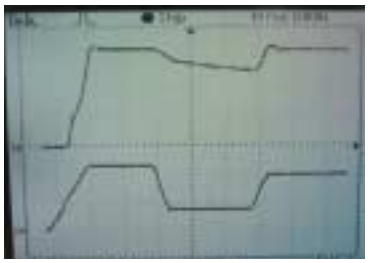

(a)

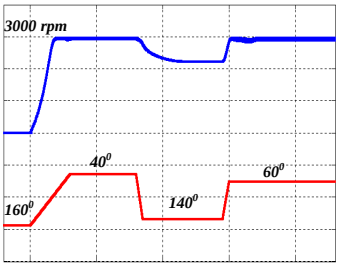

(b)

Fig. 10 Effect of TRIAC firing angle on motor speed
(a) Experimental (b) Simulated
(upper) ω[1000rpm/div] (lower) π-α[90^0/div]
(horizontal) t[5 Sec/div]

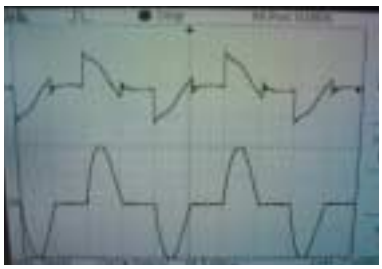

(a)

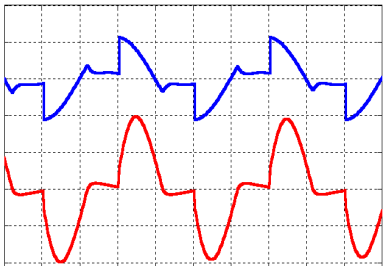

(b)

Fig. 11 Controlled supply voltage and current using a TRIAC
(a) Experimental (b) Simulated
(upper) v_{as} [200V/div] (lower) i_{as} [0.5A/div]
(horizontal) t [5m Sec/div]